Energy transfer in samarium-doped calcium tungstate crystals*

Michael J. Treadaway† and Richard C. Powell
Department of Physics, Oklahoma State University, Stillwater, Oklahoma 74074
(Received 4 September 1974)

Results of an extensive investigation of the optical properties of $CaWO_4:Sm^{3+}$ are reported. Absorption, fluorescence, and excitation spectra and pulsed fluorescence measurements were obtained at temperatures from below 8 K to room temperature on an undoped single crystal and crystals containing samarium concentrations ranging between 0.01% and 1.0%. An empirical energy-level diagram is determined for trivalent samarium in this host and the existance of several different nonequivalent crystal-field states is established. It is found that host-sensitized energy transfer to the samarium occurs in varying degrees from all four of the lowest excited states of calcium tungstate and the efficiency of transfer is different for different crystal-field sites. The ratios of the integrated fluorescence intensities and decay times were measured and from these the temperature and doping concentration dependences of the energy transfer rate were found for excitation in the different host excited states. A model is proposed to explain the results which is based on energy transfer from self-trapped excitons at low temperatures and thermally activated exciton hopping migration to activator-induced host traps at high temperatures. This model predicts the correct dependences for all of the observed data. Quantitative estimates indicate that exchange is somewhat stronger than dipole-dipole interaction for both migration and transfer and the exciton diffusion coefficient is found to be on the order of 10^{-7} cm^2 sec^{-1}.

I. INTRODUCTION

Although it has been known for many years that electronic excitation energy in tungstates, molybdates, vanadates, and similar crystals can be transferred to impurity ions, the process of "host-sensitized" energy transfer has not been well characterized and understood. This physical process has practical importance since it serves to quench the luminescence emission of pure phosphors through the transfer of excitation energy to "sinks" or it can be used to enhance the pumping of rare-earth or other impurity-based phosphors. We report here the results of an extensive investigation of the optical properties of $CaWO_4:Sm^{3+}$. Absorption, fluorescence, and excitation spectra and pulsed fluorescence measurements were made and the integrated fluorescence intensities and decay times were obtained as a function of temperature and samarium concentration. A model is proposed to explain host-sensitized energy transfer in this system and the population-rate equations based on this model are shown to qualitatively predict the observed temperature and concentration dependences of the fluorescence intensities and lifetimes. Quantitative estimates are made to determine the parameters characterizing the energy-transfer mechanisms.

A. Review of theoretical considerations

Before discussing the specific case which was investigated, it is useful to summarize the general concepts of energy-transfer theory which will be used later in the interpretation of the results. The primary question to be answered is whether the energy transfer takes place by a single- or multistep process. In the first case the sensitizer ion which absorbs the excitation energy transfers it to the activator ion while in the second case the energy migrates from one host ion to another before being transferred to an activator.

The two most important mechanisms for single-step energy transfer are dipole-dipole and exchange interaction. The energy-transfer rates between two isolated ions for these two mechanisms are given by[1–3]

$$p_{dd} = (\tau_S^0)^{-1} (R_0/R)^6, \tag{1}$$

$$p_{ex} = (\tau_S^0)^{-1} \exp[(2R_0/L)(1 - R/R_0)], \tag{2}$$

where the critical energy transfer distance for dipole-dipole interaction can be written

$$R_0 = [5.86\times10^{-25} (\Omega\phi_S^0)/(n\bar{\nu}_{SA})^4]^{1/6}. \tag{3}$$

Here ϕ_S^0 is the quantum efficiency of the sensitizer in the absence of energy transfer, Ω is the overlap integral of the absorption spectrum of the activator and emission spectrum of the sensitizer, n is the index of refraction, $\bar{\nu}_{SA}$ is the average wave number in the region of spectral overlap, and L is an "effective Bohr radius." R is the separation between the sensitizer and activator ions and τ_S^0 is the fluorescence decay time of the sensitizer in the absence of energy transfer. The numerical factor in Eq. (3) is for unit consistency and includes a factor of $\frac{2}{3}$ for the average angular dependence of randomly oriented dipoles. No simple estimate can be obtained for the R_0 due to exchange interaction since it involves the wave-function overlap.

For a random distribution of sensitizers and acti-

vators the dipole-dipole and exchange energy transfer rates will be given by

$$P_{dd} = \tfrac{1}{2}[\pi/(t\tau_S^0)(C_A/C_0)]^{1/2}, \tag{4}$$

$$P_{ex} = \frac{C_A}{C_0\gamma^3}\frac{d}{dt}g\frac{e^\gamma t}{\tau_S^0}, \tag{5}$$

where C_A is the activator concentration and $g(z)$ is a function which can be expressed as an absolutely convergent infinite series in z. Also,

$$\gamma = 2R_0/L, \tag{6}$$

$$C_0 = 3/4\pi R_0^3. \tag{7}$$

All of the energy-transfer rates discussed above exhibit only a weak dependence on temperature which is contained in the spectral overlap integral. The isolated pair transfer rates in Eqs. (1) and (2) are independent of activator concentration, whereas the rates for random distributions of ions given by Eqs. (4) and (5) depend linearly on C_A. Similarly, the isolated pair transfer rates are not time dependent, whereas the dipole-dipole transfer rate in Eq. (4) varies as $t^{-1/2}$ and the exchange interaction rate in Eq. (5) has a complicated time dependence contained in the function $g(e\gamma t/\tau_S^0)$.

In a multistep transfer process the migrating energy can be treated in the quasiparticle formalism as an exciton. The energy transfer rate in this case is given by[4]

$$k = 4\pi D R_A C_A, \tag{8}$$

where R_A is the effective trapping radius for the exciton at the activator ion and the diffusion constant can be expressed in terms of the diffusion length l as

$$D = l^2/2\tau_s^0. \tag{9}$$

In many cases the migration is best described as a nearest neighbor random walk and the diffusion coefficient can be related to microscopic parameters characterizing the walk

$$D = a^2/6t_h. \tag{10}$$

Here a is the lattice spacing and t_h is the average hopping time for the exciton. In this case each hop in the random walk can be considered as a single-step energy-transfer process described above and the hopping time is just the reciprocal of the transfer rate given by either Eq. (1) or (2).

The energy-transfer rate for exciton migration given in Eq. (8) is independent of time and varies linearly with activator concentration. The temperature dependence is contained in the diffusion coefficient and depends on the physical process limiting the mean free path of the exciton. For an incoherent hopping motion[5]

$$D = D_0 e^{-\Delta E/k_B T}, \tag{11}$$

where ΔE is an activation energy needed for each hop and k_B is Boltzmann's constant.

The energy-transfer rate is determined experimentally by measuring the ratio of the fluorescence lifetimes in the doped and undoped samples and the ratio of the integrated fluorescence intensities of the activator and sensitizer ions. The temperature, activator concentration, and time dependence of the results can then be used to determine the mechanism of energy transfer and characterize the process in terms of the parameters of the specific model.

B. Summary of $CaWO_2$ results

The optical properties of calcium tungstate are of interest because of its importance as a phosphor and laser host material. $CaWO_4$ has a scheelite structure with WO_4^{2-} molecular ions loosely bound to Ca^{2+} cations.

We recently reported the results of an investigation of the spectroscopic properties of undoped calcium tungstate.[6] Four different excitation bands were identified and assigned to transitions between the molecular orbital levels of the WO_4^{2-} tetrahedral ion split by the crystal field of S_4 site symmetry. Fluorescence emission was identified from each of the four excited states. It consisted of one broad band peaking near 4400 Å, two broad bands peaking near 5200 Å and a sharp zero-phonon line at 3680 Å. A second zero-phonon line was also observed and attributed to fluorescence from "traps" consisting of tungstate molecules located near lattice defects. The temperature dependences of the relative fluorescence intensities and decay times were measured and a model was proposed to explain the results. In this model the fluorescence at 10 K is associated with self-trapped excitons. As temperature is increased the excitons become mobile and migrate through the lattice. By 100 K the migration is so efficient that many of the excitons become trapped and a majority of the observed fluorescence is from perturbed tungstate sites.

Since the concentration of host traps can not be determined directly, no quantitative estimates could be made on the diffusion length of excitons in the pure sample. By investigating samples doped with fluorescing impurities of known concentration, it should be possible to verify the proposed model and quantitatively characterize the exciton migration.

II. EXPERIMENTAL

A. Samples and apparatus

Four good single-crystal boules of calcium tungstate doped with trivalent samarium in concentrations of 0.00, 0.01, 0.10, and 1.00 at.% were obtained from Airtron, Inc. They were charge compensated with Na^+ in concentrations equivalent to that of the samarium. All boules were grown along

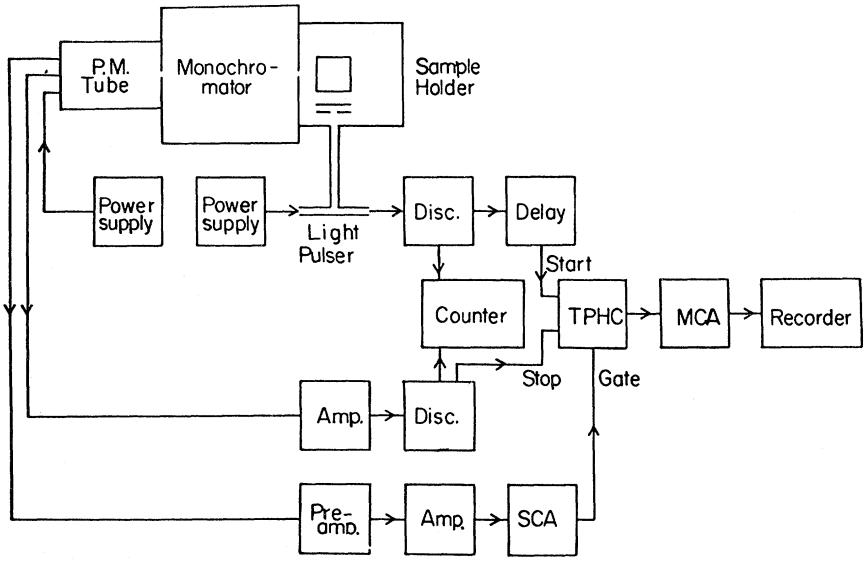

FIG. 1. Single-photon counting coincident technique for measuring fluorescence lifetimes.

the crystallographic *a* axis and samples of about 3-mm thickness were cut perpendicular to this direction. The samples were mounted on the cold finger an Air Products Displex cryogenic refrigerator capable of continuously varying the temperature from room temperature to about 7 K.

The absorption spectra were obtained on a Cary 14 spectrophotometer. Excitation spectra of the undoped sample were obtained using a 150-W xenon lamp. Excitation spectra of doped samples and all fluorescence spectra were obtained using an AH6 1000-W high-pressure mercury lamp. A Spex Minimate monochromator was used to select the excitation wavelength. The sample fluorescence was chopped and focused onto the entrance slits of a Spex 1-m monochromator and detected by a cooled RCA C31034 photomultiplier tube. The signal was amplified by a PAR lock-in amplifier and displayed on a strip-chart recorder.

Fluorescence lifetime measurements were made using single photon counting techniques. Two methods were employed. For fluorescence signals with lifetimes less than 150 μsec (such as for WO_4^{2-}) the coincident pulse-height analysis system shown in Fig. 1 was used. The excitation source was a free running spark gap oscillator which produces pulses with a half-width of approximately 5 nsec. The fluorescence was detected by an RCA 8850 photomultiplier tube and the rest of the electronic components are made by Ortec. For fluorescence signals with lifetimes greater than 0.5 msec (such as for Sm^{3+}) multichannel scaling techniques were used. For this case a xenon corporation "nanopulser" was used as an excitation pulse and the fluorescence was detected by an RCA C31034 photomultiplier tube.

B. Observed spectra

Figure 2 shows the absorption spectrum of a 23-mm-thick sample of calcium tungstate containing 1-at.% Sm^{3+} at room temperature. This spectrum was obtained using unpolarized light with the light path along the crystallographic *a* axis. It appears

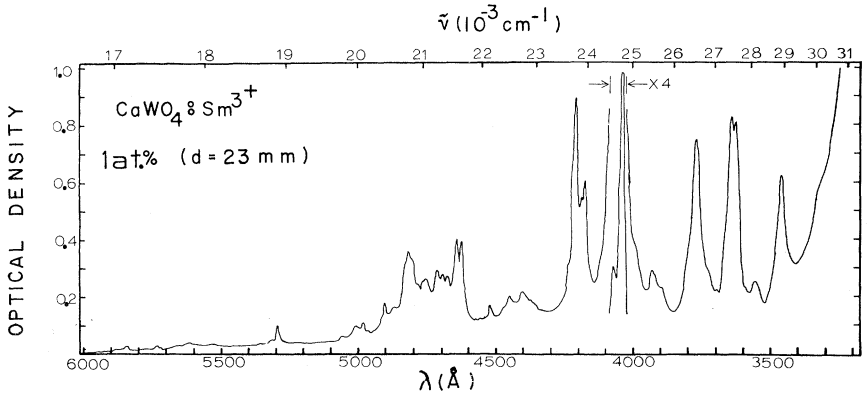

FIG. 2. Absorption spectrum of calcium tungstate with 1.0-at.% Sm^{3+} at room temperature.

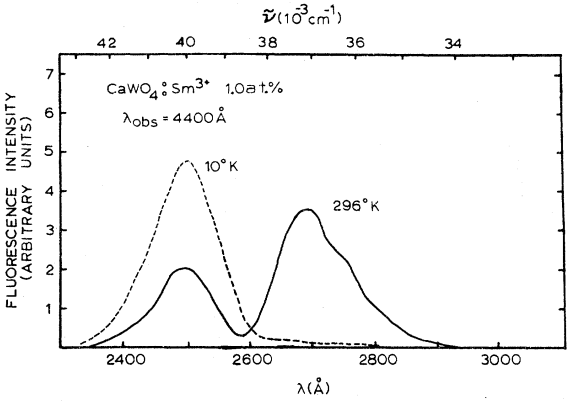

FIG. 3. Excitation spectra of the tungstate fluorescence at 4400 Å for $CaWO_4$: Sm^{3+} (1.0 at.%) at two temperatures. Correction for system response would enhance the high-energy band with respect to the low-energy band.

to be the superposition of the intrinsic absorption of the host and the impurity spectrum. The former exhibits a sharp absorption edge below 3400 Å and a long tail which decreases almost continuously out to about 5000 Å with a small peak occurring around 3900 Å.[6] The samarium absorption is a series of about 58 sharp lines between 3300 and 6000 Å with the most intense lines occurring near 4050 Å. Polarization measurements show little effect on the relative intensities of the lines. In general the optical densities appear to be lower for polarization parallel to the *c* axis than for perpendicular polarization.

The excitation spectrum for the host-crystal fluorescence observed at 4400 Å is shown in Fig. 3 for the 1-at.% sample at 10 K and room temperature. A similar spectrum is exhibited by the more lightly doped samples except that the 2700-Å band has a greater intensity relative to the 2500-Å band for lower concentrations. This is similar to the spectrum observed for the undoped sample but the two bands were not as well resolved.[6] At low temperatures the 2500-Å band increases in intensity while the 2700-Å band decreases. This change is dependent on the samarium concentration, being present but less pronounced in the more lightly doped and undoped samples. In the pure crystal two weak bands peaking near 3000 and 3550 Å could also be observed at 10 K. The latter band can not be seen in any of the doped samples where as the former band can be seen only very weakly in the 0.01% sample.

The excitation spectra obtained by observing the samarium fluorescence at 6463 Å at room temperature and 10 K in the 1.0-at.% sample are shown in Fig. 4. Comparison with the absorption spectrum of Fig. 1 indicates that excitation bands at wavelengths longer than 3300 Å are the result of direct excitation of the Sm^{3+} ions. These intrinsic samarium bands exhibit a general increase in intensity as temperature is lowered. The bands at wavelengths shorter than 3300 Å are the result of excitation of the samarium ions via energy transfer from the calcium tungstate host. The two highest-energy bands are the same ones observed in the tungstate excitation spectra shown in Fig. 3 and in general exhibit the same concentration-dependent variation with temperature. The weak broad-band peaking near 3000 Å in the tungstate excitation spectra is more intense in the samarium exciton spectra and appears to be resolved into two distinct peaks near 3000 and 3150 Å. At 10 K, the 3150-Å peak is more intense for all three samarium concentrations. However, at room temperature this peak is more intense for the 1.0-at.% sample, the two peaks have approximately the same intensities for the 0.1-at.% sample, and the 3000-Å peak has the greater intensity for the 0.01-at.% sample.

Figure 5 shows the four regions of the directly pumped Sm^{3+} fluorescence spectra exhibiting the most intense lines. Many smaller peaks are observed inbetween these regions and a total of 83 fluorescence lines can be identified for the heavily doped sample at 8 K. No relative changes in intensity occur for different polarizations. The relative intensity scales are arbitrary for each of the four regions. On an absolute scale the biggest line in the region designated as $^6H_{5/2}$ would have the same intensity as the biggest line in the $^6H_{11/2}$ region, and the most intense lines in the other two regions are about 1.75 times greater.

Figure 6 shows the fluorescence spectrum of

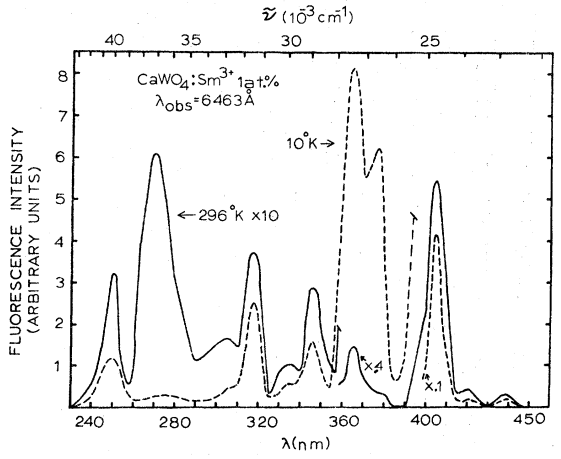

FIG. 4. Excitation spectra of the samarium fluorescence at 6463 Å for $CaWO_4$: Sm^{3+} (1.0 at.%) at two temperatures. Correction for system response would enhance the high-energy bands with respect to the low-energy bands.

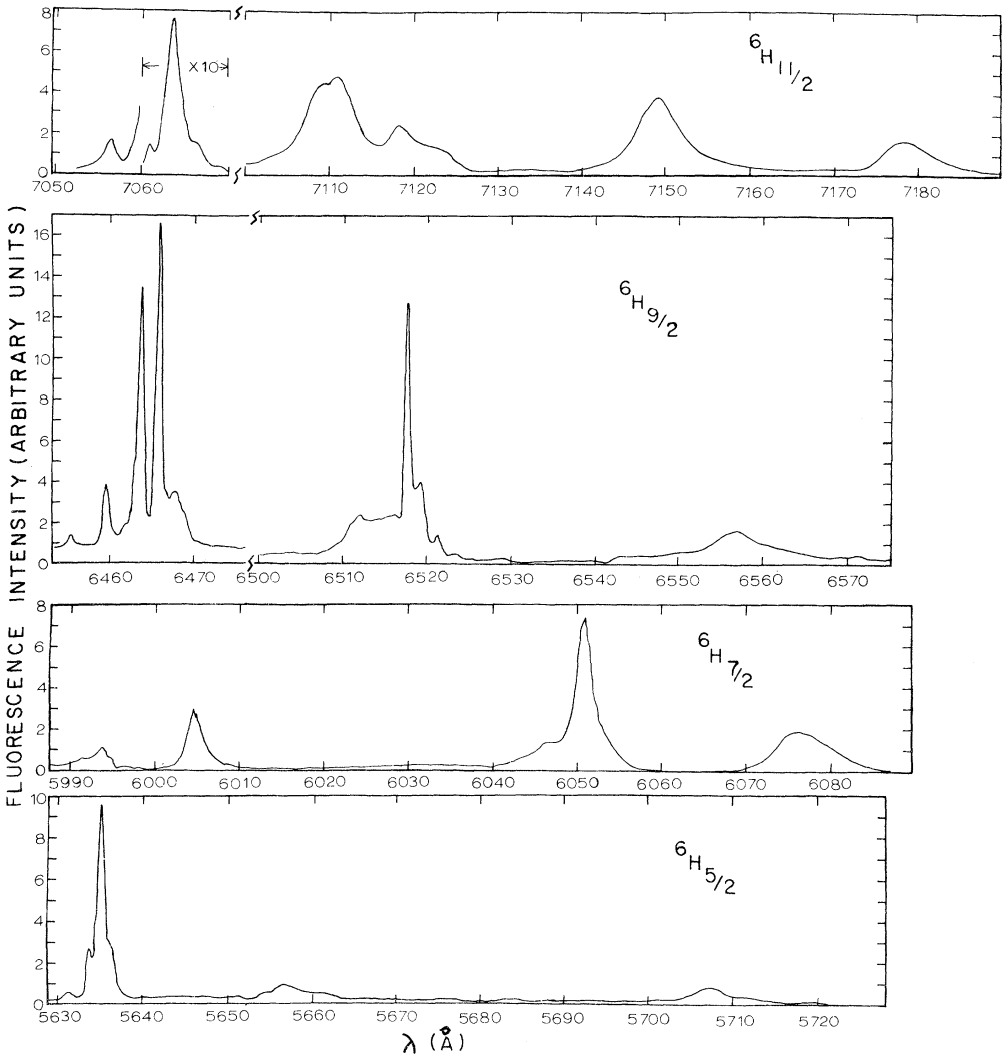

FIG. 5. Four regions of the fluorescence spectrum of $CaWO_4$: Sm^{3+} (1.0 at.%) at about 8 K for 4150-Å excitation.

$CaWO_4$: Sm^{3+} excited at 2650 Å for both the 0.1-at.% samples. Both the broad band tungstate fluorescence and the sharp emission lines of trivalent samarium can be observed. (The lowest-energy set of Sm^{3+} lines is not shown in this figure.) The dips in the broad band near 4050 and 4190 Å correspond to regions of high samarium absorption. Unlike the results obtained on the undoped sample,[6] the 4400-Å emission band was observed at all temperatures for all wavelengths of excitation. Neither of the longer wavelength bands nor the zero-phonon lines could be observed in samples containing samarium. For 2400-Å excitation of the lightest-doped sample, no samarium fluorescence can be observed, whereas for 3150-Å excitation tungstate fluorescence could be observed only for the lightest-doped sample at low temperatures. The relative intensities of the lines in the complicated samarium spectra change

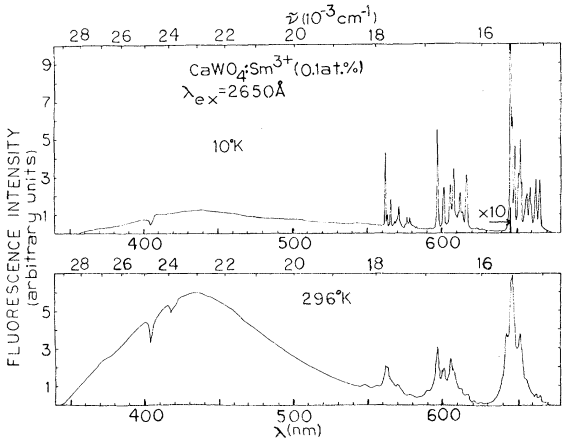

FIG. 6. Fluorescence spectra of $CaWO_4$: Sm^{3+} (0.1 at.%) at two temperatures for 2650-Å excitation.

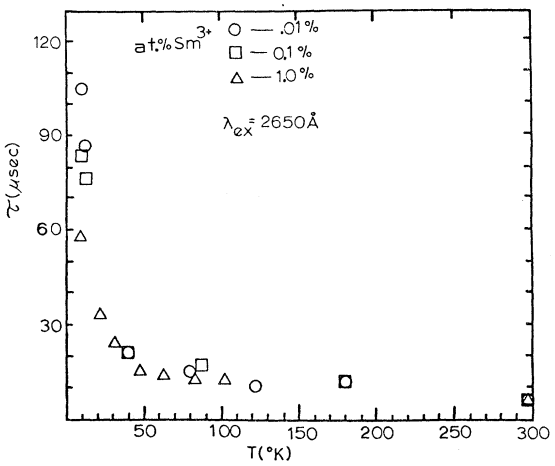

FIG. 7. Temperature dependence of the tungstate lifetime in $CaWO_4$: Sm^{3+} for 2650-Å excitation.

with wavelength of excitation, concentration, and temperature.

It should be noted that the spectra shown in Figs. 3–6 have not been corrected for the spectral response of the system. This correction would have very little effect on the fluorescence spectra but would cause the high-energy bands in the excitation spectra to be enhanced considerably with respect to the low-energy bands.

C. Pulsed fluorescence results

The decay time of the samarium fluorescence was measured to be about 0.85 msec at room temperature for all three samples. Within experimental error this result was obtained both for direct pumping at 4150 Å and for pumping through the host at 2400, 2650, and 3150 Å. As temperature was lowered the decay time decreased slightly to about 0.60 msec at 8 K. All decays were purely exponential with no observed rise times.

The tungstate fluorescence lifetimes in the doped samples exhibits a similar temperature dependence as seen in the undoped crystal.[6] Between about 8 and 80 K there is a sharp decrease in the decay time as shown in Fig. 7 for 2650-Å excitation. It then remains constant up to about 200 K and decreases slightly by room temperature. A similar dependence is observed for 2400-Å excitation but no signal could be detected for 3150-Å excitation. All decay curves were pure exponentials with no initial rises.

III. INTERPRETATION OF RESULTS

A. Energy levels for Sm^{3+}

The observed spectra of Sm^{3+} in calcium tungstate is due to transitions between energy levels of the $4f^5$ configuration. Several attempts have been made to calculate the free-ion energy levels of trivalent samarium[7–9] and the most recent results[9] indicate that the lowest-lying fluorescent state is $^4F_{5/2}$. The terminal levels for the fluorescent transitions are the various multiplets of the ^6H term with the ground state being $^6H_{5/2}$.

The trivalent samarium ions probably substitute for Ca^{2+} ions in calcium tungstate because of ionic-

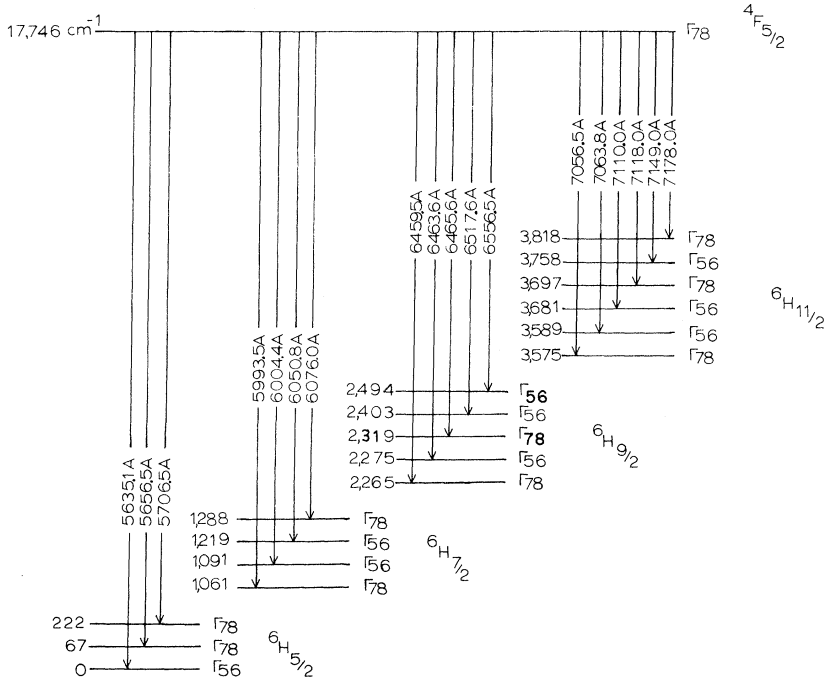

FIG. 8. Empirical energy-level diagram for Sm^{3+} in calcium tungstate.

size considerations. This site is surrounded by eight WO_4^{2-} ions giving a crystal field of S_4 symmetry which splits the multiplets into their Stark components. There are four possible types of crystal-field levels, Γ_5, Γ_6, Γ_7, and Γ_8. These occur in Kramers degenerate pairs labeled Γ_{78}. Na^+ ions provide the necessary charge compensation which is mostly nonlocal although some locally compensated Sm^{3+} sites probably are present.[10] Nearest-neighbor impurities would lower the samarium site symmetry to C_1 but this would not cause further splitting of the Kramers degenerate levels.

The observed spectral lines may be due either to magnetic dipole or forced electric-dipole transitions which have different selection rules for polarized light. The fact that no polarization effects were observed essentially implies that both types of transitions are taking place with approximately the same order of magnitude.

An empirical energy-level diagram for Sm^{3+} in $CaWO_4$ is shown in Fig. 8. This was obtained from the directly pumped samarium fluorescence spectrum at low temperatures for the lightest-doped sample where the minimum number of lines were observed. Each of the multiplets of the ^6H term should split into $J+\frac{1}{2}$ crystal-field level and, if all the fluorescence originates from the same metastable level, a line should appear in the spectrum for a transition to each of these levels. The correct number of major lines was observed. The designations for the crystal-field states were obtained by noting that within each set of lines the number of the most intense transitions equaled the number of Γ_{56} states predicted by symmetry considerations. The metastable level is arbitrarily assigned to Γ_{78} since this makes electric dipole transitions to the Γ_{56} levels allowed in both polarizations.

The extraneous lines observed in the spectra may be due to several causes including nonequivalent crystal-field sites for the samarium ions, emission from higher excited metastable states, and vibronic transitions.

B. Energy-transfer model

The existence of host sensitized energy transfer in the $CaWO_4:Sm^{3+}$ system is explicitly demonstrated by the excitation spectra such as that shown in Fig. 4. Samarium fluorescence is excited by pumping in all of the host absorption bands at both high and low temperatures. It appears that the two low-energy excitation bands are more efficient in transferring energy to the samarium than the high-energy bands. Also, the fluorescence spectra indicate that the levels giving rise to the 5200-Å fluorescence band seen in undoped calcium tungstate are more efficiently quenched by the presence of samarium than those giving rise to the 4400-Å band since the former can not be seen at all in the doped samples.

To investigate the temperature dependence of the energy transfer it is most reliable to use the data obtained with 2400-Å excitation. For the other two excitation wavelengths which were used, radiationless processes between excited states in the tungstate ions take place above about 130 K.[6] As an example, consider the results obtained for 2650-Å excitation. In the undoped sample for this excitation the fluorescence band shifted to shorter wavelengths and the integrated intensity increased as temperature was raised above about 130 K. In the doped sample the long wavelength band is never observed and as temperature is increased above 130 K the tungstate intensity increases rapidly but the samarium intensity remains approximately constant. Thus, it appears that the longer-wavelength tungstate fluorescence is quenched by the presence of the samarium but this results in a radiationless loss of energy and not samarium fluorescence. This is substantiated by the decrease in the intensity of the 2700-Å excitation band with decreasing temperature as shown in both Figs. 3 and 4.

The quenching of the fluorescence decay time of the sensitizer and the ratio of the integrated intensities of the activator and sensitizer can both generally be used to obtain the rate of energy transfer. These quantities are shown in Fig. 9 plotted as a function of activator concentration for two different temperatures. Figure 10 shows the same quantities plotted as a function of temperature for the sample containing 0.1-at.% samarium. Qualitatively, similar results are obtained for both 2400- and 2650-Å excitation wavelengths except that above 130 K the intensity ratios for 2650-Å excitation are affected by radiationless quenching processes discussed

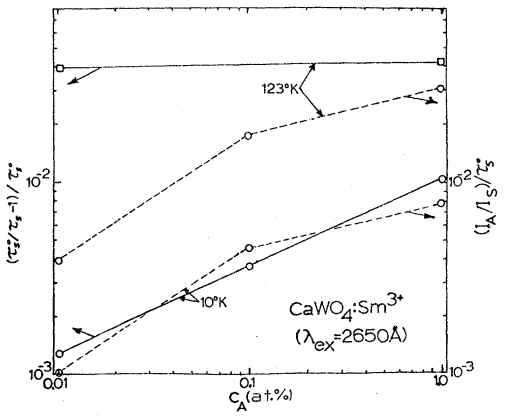

FIG. 9. Ratios of the fluorescence intensities and decay times as a function of samarium concentration for 2650-Å excitation. τ_s^0 and τ_s are the lifetimes in the undoped and doped samples, respectively, while I_A is the integrated fluorescence intensity of the activator (Sm^{3+}) and I_S is the integrated fluorescence intensity of the sensitizer ($CaWO_4$).

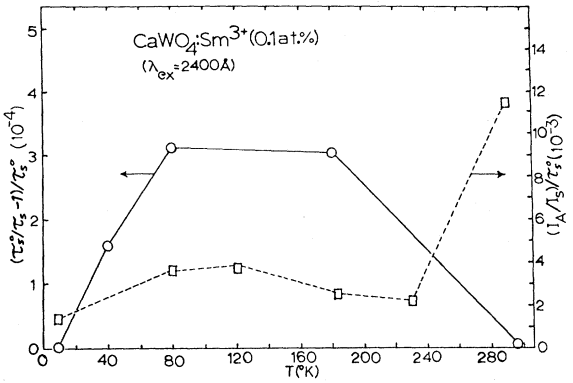

FIG. 10. Ratios of the fluorescence intensities and decay times as a function of temperature for 0.1-at.% samarium concentration with 2400-Å excitation. (The ratios are the same as those described in Fig. 9.)

above. Near 10 K both lifetime and intensity measurements indicate that the energy-transfer rate increases with increasing samarium concentration. Above 100 K, intensity ratios still show the energy-transfer rate to increase with samarium concentration, whereas the lifetime quenching is independent of concentration. Both intensity and lifetime ratios show an increase in the energy-transfer rate between 10 and 80 K and an approximately constant rate between 80 and 150 K. The lifetime ratios show a decrease in the energy-transfer rate at higher temperatures while the intensity ratios decrease at first and then increase sharply near room temperature.

Figure 11 shows a proposed model for explaining host sensitized energy transfer in this system. It correctly predicts the experimental observations described above and is consistent with the model proposed previously to explain the results obtained on undoped calcium tungstate.[6] A concentration of excitons n_s is created at a rate W. At low temperatures the excitons become self-trapped with an activation energy ΔE. From this level they can either fluoresce with a decay rate B_S (assumed to be the same for both trapped and untrapped excitons) or transfer their energy to activators by some resonance process whose rate is designated as $F(C_A)$. At high temperatures the excitons can overcome the activation energy and undergo a thermally activated hopping migration. During this migration the excitons can decay with a rate B_S, become trapped at activators, or become trapped at host trapping sites. For the doped sample, we consider two types of host traps, intrinsic defect sites whose concentration is C_X, and defect sites surrounding the activators due to their induced perturbation of the host lattice. The concentration of the latter type of traps will be approximately the same as the activator concentration C_A. The exciton trapping rates for activators, induced traps, and intrinsic traps are $k_A C_A$, kC_A, and kC_X, respectively. The excited-state concentrations of these sites are n_A, n_{XA}, and n_X. The excited activators have a fluorescence decay rate of B_A while both types of trapping sites are assumed to have the same fluorescence decay rate of B_X. The activator induced traps can also transfer their energy to the neighboring activator with a rate of q_A. The specific nature of the energy transfer and trapping parameters will be discussed later.

The rate equations for the excited state populations in this model can be written

$$\dot{n}_S(t) = -[F(C_A) + kC_X + kC_A + k_A C_A + B_S] \times n_S(t) + W(t), \tag{12}$$

$$\dot{n}_X(t) = -B_X n_X(t) + kC_X n_S(t), \tag{13}$$

$$\dot{n}_{XA}(t) = -(B_X + q_A) n_{XA}(t) + kC_A n_S(t), \tag{14}$$

$$\dot{n}_A(t) = -B_A n_A(t) + q_A n_{XA}(t) + [k_A C_A + F(C_A)] n_S(t), \tag{15}$$

where it has been assumed that there is no direct excitation of activators or traps. The observed fluorescence intensities for each type of excited state will be the radiative decay rate multiplied by the population of the level. The observed tungstate fluorescence in this case is a combination of the emission from normal host sites, intrinsic host trpas, and activator-induced traps.

First consider the predictions of the model for host lifetime quenching. The rate equations can be solved for δ-function excitation and the exciton and trap emissions combine to give the time dependence of the total tungstate fluorescence intensity

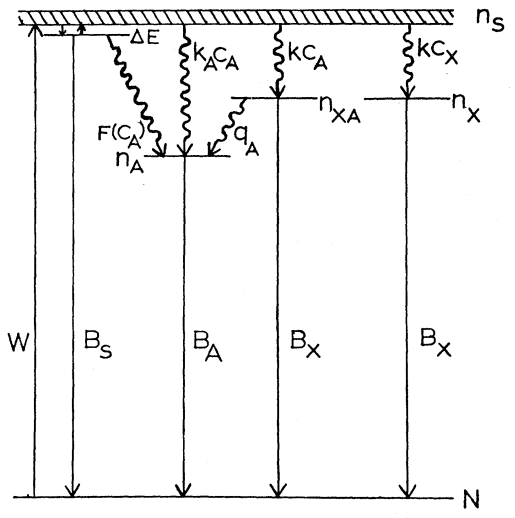

FIG. 11. Proposed model for energy in $CaWO_4$: Sm^{3+}. (See text for explanation of the symbols.)

$$I_H(t) = n_S(0)\Bigg[\Bigg(B_S' + \frac{B_X' C_X k}{B_X - B_S - kC_X - kC_A - k_A C_A - F(C_A)} + \frac{B_X' C_A k}{B_X + q_A - B_S - kC_X - kC_A - k_A C_A - F(C_A)}\Bigg)$$
$$\times \exp\{-[B_S + kC_X + kC_A + k_A C_A + F(C_A)]t\} - \frac{B_X' C_X k}{B_X - B_S - kC_X - kC_A - k_A C_A - F(C_A)} \exp(-B_X t)$$
$$- \frac{B_X' C_A k}{B_X + q_A - B_S - kC_X - kC_A - k_A C_A - F(C_A)} \exp[-(B_X + q_A)t]\Bigg]. \quad (16)$$

Here the primes indicate radiative decay rates. In order to obtain the observed results it is necessary to assume that $k_A \ll k$ so that direct trapping by activators is negligible compared to trapping at activator-induced host traps.

Since the expression in Eq. (16) is very complicated, it is useful to treat three temperature regions separately where simplifications can be made. First consider the results for very low temperatures of 10 K or below where the self-trapped excitons can not gain enough thermal energy to be mobile. For this case k is zero and Eq. (16) reduces to

$$I_H(t) = B_S' n_S(0)\, e^{-[B_S + F(C_A)]t}. \quad (17)$$

The measured fluorescence decay time is given by

$$\tau_S = [B_S + F(C_A)]^{-1}. \quad (18)$$

As temperature is increased slightly above 10 K the excitons become mobile. k is small but no longer zero. The majority of the observed fluorescence is from the normal host sites and therefore the first coefficient in the first term of Eq. (16) still dominates and the lifetime becomes approximately

$$\tau_S = [B_S + kC_X + kC_A + F(C_A)]^{-1}. \quad (19)$$

Thus, as temperature is increased the host lifetime decreases as k increases.

As the temperature is increased further, the energy migration rate to traps becomes very fast so that $kC_A + kC_X \gg B_S, (B_X + q_A)$. Then the first exponent in Eq. (16) becomes negligible after short times so the host intensity is described by

$$I_H(t) = n_S(0)\Bigg(\frac{B_X' C_X k}{kC_X + kC_A}\, e^{-B_X t} + \frac{B_X' C_A k}{kC_X + kC_A}\, e^{-(B_X + q_A)t}\Bigg). \quad (20)$$

If the activator concentration is much greater than that of the intrinsic host traps, this reduces to

$$I_H(t) = B_X' n_S(0)\, e^{-(B_X + q_A)t} \quad (21)$$

and the lifetime is given by

$$\tau_S = (B_S + q_A)^{-1}. \quad (22)$$

Equations (18), (19), and (22) can be used to explain qualitatively the temperature and concentration dependences of the lifetime quenching shown in Figs. 9 and 10. At 10 K the lifetime ratio plotted in these figures gives $F(C_A)$, the resonant-energy-transfer rate from self-trapped excitons to activators. This should have a very weak temperature dependence contained in the spectral overlap integral and a strong concentration dependence depending on the interaction mechanism as discussed in Sec. I.

As temperature is raised, the migration and trapping rates become important. These depend linearly on the concentration of activators and intrinsic host traps. The temperature dependence is contained in the diffusion coefficient and for thermally activated hopping is simply an exponential factor as given by Eq. (11).

At temperatures above about 80 K, migration is fast enough that much of the host fluorescence comes from traps and for $C_A \gg C_X$ most of it comes from activator-induced host traps. The lifetime ratio obtained from Eq. (22) just gives q_A, which is the resonant-energy-transfer rate from activator-induced host traps to activators. This will have a very weak temperature dependence contained in the spectral overlap integral and no concentration dependence since it always involves nearest-neighbor interactions as discussed in Sec. I.

Now consider the model predictions for relative fluorescence intensities. For this case Eqs. (12)–(15) can be solved for continuous excitation to give the steady-state populations

$$n_S = WN_S/[B_S + kC_X + kC_A + k_A C_A + F(C_A)], \quad (23)$$
$$n_X = (kC_X/B_X) n_S,$$
$$n_{XA} = [kC_A/(B_X + q_A)] n_S, \quad (24)$$
$$n_A = (n_S/B_A)[q_A kC_A/(B_X + q_A) + k_A C_A + F(C_A)]. \quad (26)$$

Then the tungstate and samarium fluorescence intensities are given by

$$I_H = n_S\Bigg(B_S' + \frac{B_X'}{B_X} kC_X + \frac{B_X'}{B_X + q_A} kC_A\Bigg), \quad (27)$$

$$I_A = n_S \frac{B_A'}{B_A}\Bigg(\frac{q_A kC_A}{B_X + q_A} + k_A C_A + F(C_A)\Bigg) \quad (28)$$

and the fluorescence intensity ratio can be written

$$\frac{I_A}{I_H} = \frac{\phi_A[q_A kC_A/(B_X + q_A) + k_A C_A + F(C_A)]}{B_S' + \phi_X^0 kC_X + \phi_X kC_A}. \quad (29)$$

Here ϕ_X^0 and ϕ_X are the quantum efficiencies of the calcium tungstate in the undoped and doped samples, respectively, above 100 K where most of the host fluorescence comes from traps, ϕ_A is the quantum efficiency of the samarium which can be taken to be approximately one. Also we assume $k_A \ll k$ as above. Again let us consider the low- and high-temperature limits separately. At 10 K where k is very small, Eq. (29) becomes

$$I_A/I_H \approx F(C_A)/B_S' = [F(C_A)/\phi_S^0]\,\tau_S^0. \tag{30}$$

Here we have made use of the relationship between B_S' and the observed host-fluorescence decay time in this temperature range given in Ref. 6. Above 100 K where kC_A becomes large, Eq. (29) becomes

$$\frac{I_A}{I_H} = \frac{q_A kC_A/(B_X + q_A)}{\phi_X^0 kC_X + \phi_X kC_A} = \frac{q_A \tau_S C_A}{\phi_X^0 C_X + \phi_X C_A} \tag{31}$$

where use has been made of Eq. (22) in the last expression which is valid for $C_X < C_A$.

The above considerations predict that the quantity $(I_A/I_H)\tau_S^0$ plotted in Figs. 9 and 10 will depend on activator concentration linearly or greater at low temperatures and less than linearly at high temperatures. For all concentrations of activators this quantity should increase with temperature above 10 K as exciton migration increases and become constant above about 80 K. This is consistent with experimental observations.

There is an apparent discrepancy in the temperature dependence of the energy-transfer rate above 250 K predicted by lifetime and intensity measurements as seen in Fig. 10. This can be attributed to radiationless quenching processes not included in the proposed model. The existance of radiationless quenching is substantiated by the decrease in the fluorescence intensities and decay times observed in the undoped sample in this temperature range.[6] For the doped samples it is found that the samarium intensity increases as the tungstate intensity decreases above 250 K, indicating an increase in energy transfer. However, the increase in samarium fluorescence is not proportional to the decrease in the tungstate fluorescence implying an additional loss due to radiationless processes. The tungstate fluorescence decay time is found to decrease more rapidly with temperature in this range in the undoped sample than in the doped samples. Since Eq. (22) shows that the measured lifetime in the doped sample is that of activator induced host traps, whereas in the undoped sample the lifetime is that of intrinsic host traps, the data seem to indicate that the latter are affected more by radiationless quenching than the former. This explains the apparent decrease in the lifetime ratios near room temperature seen in Fig. 10. The intensity ratio plotted in this figure depends on the inverse of this lifetime ratio as indicated by Eq. (31) thus the observed increase is much greater than the true increase in the energy-transfer rate.

The mechanisms for energy transfer in the high- and low-temperature limits can be determined by making a quantitative comparison between the energy-transfer rates found experimentally from fluorescence lifetime and intensity measurements and the theoretical expressions given in Eqs. (1)–(11). The critical energy transfer distance is determined from Eq. (3) using $n = 1.92$, $\bar{\nu}_{SA} = 2.48\times10^4$ cm^{-1}, $\phi_S^0 \approx 1$, and a calculated value of the spectral overlap integral of 3.35×10^{-2} mole^{-1} cm^{-1} liter^{-1}. R_0 is found to be 3.95 Å for dipole-dipole interaction.

First consider the results above 100 K. Using the nearest-neighbor WO_4^{2-}-Ca^{2+} separation of 3.68 Å for R, the dipole-dipole energy-transfer rate is found from Eq. (1) to be 7.2×10^4 sec^{-1} for 2400-Å excitation and 6.0×10^4 sec^{-1} for 2650-Å excitation at 180 K. The energy-transfer rate for exchange interaction can be estimated by Eq. (2) using a value for R_0 similar to that found for dipole-dipole interaction and an effective Bohr radius of $L \approx 0.9$ Å which is half the W-O separation. This yields rates of 8.6×10^4 sec^{-1} and 7.2×10^4 sec^{-1} at 180 K for 2400- and 2650-Å excitation, respectively. The experimentally determined values at this temperature are 3.5×10^4 sec^{-1} and 3.7×10^4 sec^{-1} for 2400- and 2650-Å excitation as predicted by Eq. (22). The good agreement between experimentally and theoretically determined rates tends to substantiate the proposed model that at these temperatures energy transfer to samarium takes place mainly from nearest-neighbor host traps. However, the similarity of the predictions for dipole-dipole and exchange makes it impossible to unambiguously attribute the energy transfer transition to one of these interactions. The larger predicted values imply that exchange is probably the dominant mechanism.

A similar analysis can be made for the single step transfer process that takes place between self-trapped excitons and samarium ions at 10 K. Equation (4) predicts a quenching of the host fluorescence lifetime of only 0.95 for the 1-at.% sample for dipole-dipole interaction. A similarly small decrease in the lifetime ratio is predicted from exchange interaction using the calculations of Inokuti and Hirayama.[3] A much-greater quenching ratio of 0.5 is measured experimentally and this requires a value of R_0 on the order of 8.7 Å to be consistent with the predictions of dipole-dipole or exchange interaction. This implies that dipole-dipole interaction is not strong enough to account for the observed energy-transfer rate and that the very simple exchange model giving rise to Eq. (5) is also not sufficient to describe the physical situation. More exact theories of exchange and superexchange can greatly increase the theoretically predicted rate.[11]

By fitting Eqs. (8) and (11) to the experimentally determined temperature dependence for $(\tau_s^0/\tau_s - 1)/\tau_s^0$ as given by Eq. (19), a value for the exciton migration rate can be determined. This was found to be 5.5×10^{-14} cm^3 sec^{-1}. If the trapping radius R_A in Eq. (8) is taken to be the tungstate-tungstate lattice spacing of 3.68 Å, this gives a diffusion coefficient of $D = 1.2\times10^{-7}$ cm^2 sec^{-1}. The diffusion length can be determined from the relationship given in Eq. (9) and using the free exciton measured lifetime of ~17 μsec at 100 K for 2400-Å excitation this yields a value of $l = 1.2\times10^{-6}$ cm. Comparison of this value to the average separation between samarium ions in a sample containing 0.01-at.% Sm^{3+}, which is 5.7×10^{-7} cm, shows that after an exciton becomes mobile it can easily migrate far enough to find an activator with a high probability. This is consistent with the proposed model.

If a nearest-neighbor hopping model is used to describe the migration of energy, the average hopping time can be determined from Eq. (10) to be 2.1×10^{-9} sec. Theoretically, this should correspond to the energy-transfer rate between two neighboring tungstate molecules described by Eq. (1) or (2). However, it is difficult to determine a value of R_0 since the observed spectral overlap is indicative of emission from the relaxed excited state and using it predicts hopping times on the order of 0.1 msec. This shows the importance of the activation energy in increasing the resonance between the energy levels of the excited tungstate ion and its surrounding sungstate ions. It is not unreasonable to expect this to increase R_0 to 16 Å giving $t_h = 3.3\times10^{-9}$ sec for dipole-dipole interaction or to 8 Å giving $t_h = 1.7\times10^{-9}$ sec for exchange. Either of these are in good agreement with the experimentally determined hopping time.

Finally, a comparison of kC_A and q_A above 100 K for the 0.01-at.% sample shows that even for the lowest samarium concentration $kC_A \gg q_A$ by at least a factor of 2. This indicates that the limiting step in the energy transfer process is the final transfer from neighboring host traps to samarium ions as assumed in the model.

Note that it should also be possible to make quantitative estimates of energy-transfer parameters similar to those discussed above using the measured intensity ratios. However, the question of what to use for the exact values of the quantum efficiencies appearing in Eqs. (30) and (31) make it preferable to use the lifetime ratios. Rough approximations indicate that the estimates obtained from the two types of measurements are consistent.

IV. DISCUSSION AND CONCLUSIONS

The crystal-field splittings shown in Fig. 8 are similar to those seen for trivalent samarium in other hosts[8,12–19] and the average energies of the Stark manifolds correlate quite well with the positions of the lowest multiplets of the ^6H term of the free ion.[20] The spectra of other trivalent rare-earth ions in calcium tungstate also exhibit complicated structure which has made complete interpretation of the spectra impossible.[21–27]

The presence of many extraneous lines in the Sm^{3+} spectra and the observation that their relative intensities depend on samarium concentration and the wavelength of pumping, show the existence of more than one nonequivalent site for the samarium ions and imply a difference in energy transfer rate to the different types of sites. This is consistent with the assumption of the presence of activator-induced host traps and will be investigated in more detail in a later study.

The rather complicated model for energy transfer in Fig. 11 qualitatively predicts the correct temperature and activator concentration dependence for the measured fluorescence intensity and lifetime ratios of $CaWO_4:Sm^{3+}$ and is consistent with the model proposed to explain the results obtained on undoped calcium tungstate.[6] Quantitatively, the value obtained for D in this interpretation is smaller than the diffusion coefficients found for singlet excitons in organic crystals[4] and in cadmium sulfide[28] but larger than those reported for migration among rare earth sensitizers in other host crystals and glasses.[29–32] These results indicate that at high temperatures the excitons take on the order of 8500 steps in their random walk. Blasse[33] concludes from his work that only two steps between tungstate ions occur before transfer to Eu^{3+} in the system $Y_2WO_6:Eu^{3+}$ at 77 K.

The quantitative analysis of the data in the proposed model indicates that exchange interaction is somewhat stronger than dipole-dipole interaction for both energy migration and energy transfer in this system. This is consistent with the speculation given in Ref. 2 but is questioned in Ref. 33. The expression in Eq. (2) gives an estimate for the energy transfer rate in a much oversimplified picture of exchange interaction. The more sophisticated models involving superexchange[11] lead to a highly anisotropic energy-transfer rate which falls off much less rapidly with distance. For these models the number and geometry of the oxygen linkages are much more important than the sensitizer-activator separation. However, it is difficult to calculate theoretical estimates for the transfer rates in these models since the equations involve wave-function overlap integrals. This makes it important to use exact expressions for the wave functions which are generally not known. The overlaps are therefore treated as empirical fitting parameters. Thus the transfer rates calculated in the simple theory should be considered only as a lower bound to the actual magnitude of the transfer rate.

For the model described by Eqs. (12)–(15), it generally would be expected that the fluorescence decays of both the host and activators would exhibit initial rises or double exponential behavior. Instead pure exponential decays are observed for all measurements. As discussed previously,[6] this may be due to processes not included in the model such as direct excitation of activators or fast transfer to activators before relaxation of the absorbing site.

It has been shown[34] that energy transfer can take place between samarium ions at high concentrations. This can lead to a quenching of the fluorescence intensity above about 1.0-at.% Sm^{3+} and may give rise to a less than linear concentration dependence of the fluorescence intensity ratios. This interaction has not been included in the model discussed above and it may contribute to the less than linear concentration dependence shown for the fluorescence intensity ratios in Fig. 9, although Eq. (31) also predicts this.

The excitation spectra show that all four tungstate excited states transfer their energy to samarium ions and indicate that the two low-energy states transfer energy more efficiently than the two high-energy states. This is substantiated by the fact that the characteristic fluorescence emissions from the two lower-energy levels[6] cannot be observed at all in the doped samples. The fact that lifetime quenching is observed shows that transfer from the two higher levels takes place after thermal relaxation occurs in these states. The quantitative values for the energy transfer rates discussed in Sec. III represent lower bounds for the total system since the rates will be greater for the two lower levels.

Although there is some evidence in Fig. 6 of the presence of radiative reabsorption, this is not an efficient enough process to account for much of the observed energy transfer. Also the observed quenching of the tungstate fluorescence lifetimes gives proof of the presence of radiationless energy transfer.

Theories of phonon assisted energy transfer can also predict an exponential temperature dependence for the transfer rate in some cases[34–36] as observed for this system. However, in order to concurrently explain the observed concentration dependences, it is necessary to have a more complicated process such as the exciton migration to activator induced host traps as proposed here.

Much of the previous work done on energy transfer in calcium tungstate dealt with the thermal quenching of the luminescence above room temperature and no measurements have been reported below liquid-nitrogen temperature.[37,38] Also only fluorescence intensity measurements have been made; no work has been done on lifetime quenching or excitation spectra. Within the same temperature range, our results for the temperature dependence of the fluorescence intensity ratios are similar to those reported earlier. Above room temperature the fluorescence intensities are reported to decrease rapidly due to thermal quenching in the host.[37,38] The dependence of energy transfer on excitation wavelength and the fact that this varies with samarium concentration has also been noted previously.[38] The earlier model for energy transfer in this system assumed energy migration to occur only above 200 K while below this temperature energy transfer took place only if light happened to be absorbed in a tungstate ion located next to a samarium impurity. The presence of nonfluorescing traps were postulated to account for changes in the host fluorescence with temperature. Such a model cannot explain the more complete set of data we now have available on the luminescence properties of both pure and doped $CaWO_4$. It has also been proposed that the migration of self-trapped hole (V_k) centers might be responsible for energy transfer in calcium tungstate.[39] However, the lack of production of paramagnetic centers by uv radiation and the fact that such a bimolecular process should exhibit an excitation intensity dependence which is not observed, makes this improbable.

In summary, the very complicated observations of the temperature and activator concentration dependence of the fluorescence intensities, lifetimes, and excitation spectra in samarium-doped calcium tungstate over a wide temperature range extending to below 10 K, have been interpretated using a very complex model involving both direct energy transfer and hopping migration of self-trapped excitons, and both intrinsic and activator-induced host traps. Although no conclusive proof can be given for the correctness of the model, it qualitatively predicts the observed results and gives reasonable quantitative estimates for the energy transfer parameters.

ACKNOWLEDGMENTS

The authors gratefully acknowledge the assistance of Chang Hsu in obtaining some of the experimental data and of Quiesup Kim in obtaining computer fits to the fluorescence decay curves using the proposed model.

---

*Research supported by the U. S. Army Research Office, Durham, N. C.

†Present address: Intelcom Rad. Tech., 7650 Convoy Ct., Box 80817, San Diego, Calif. 92138.

[1]Th. Förster, Ann. Phys. (Leipz.) 2, 55 (1948); Z. Naturforschg. A 4, 321 (1949).

[2]D. L. Dexter, J. Chem. Phys. 21, 836 (1953).
[3]M. Inokuti and F. Hirayama, J. Chem. Phys. 43, 1978 (1965).
[4]H. C. Wolf, in *Advances in Atomic and Molecular Physics*, edited by D. R. Bates and I. Eastermann (Academic, New York, 1967), Vol. 3, p. 119.
[5]M. Trlifaj, Czech. J. Phys. 6, 533 (1956).
[6]M. J. Treadaway and R. C. Powell, J. Chem. Phys. (to be published).
[7]B. G. Wybourne, J. Chem. Phys. 36, 2301 (1962).
[8]H. E. Rast, J. L. Fry, and H. H. Caspers, J. Chem. Phys. 46, 1460 (1967).
[9]T. V. Babkina, V. F. Zolin, and E. N. Muravey, Opt. Spektrosk, 32, 1130 (1972) [Opt. Spectrosc. 32, 613 (1972)].
[10]K. Nassau, J. Phys. Chem. Solids 24, 1511 (1963).
[11]P. W. Anderson, in *Magnetism*, edited by G. T. Rado and H. Suhl, (Academic, New York, 1963), Vol. 1, p. 25.
[12]M. S. Magno and G. H. Dieke, J. Chem. Phys. 37, 2354 (1962).
[13]J. S. Prener and J. D. Kingsley, J. Chem. Phys. 38, 667 (1963).
[14]J. D. Axe and G. H. Dieke, J. Chem. Phys. 37, 2364 (1962).
[15]S. Makishima, K. Hasegawa, and S. Shionoya, J. Phys. Chem. Solids 23, 749 (1962); S. Makishima, H. Yamamoto, T. Tomotsu, and S. Shionoya, J. Phys. Soc. Jpn. 20, 2147 (1965).
[16]Yu. V. Voronov and V. L. Levshin, Izv. Akad. Nauk. SSSR Ser. Fiz. 29, 503 (1965).
[17]S. Larach, *Proceedings of the International Conference on Luminescence* (Akademiai Kiado, Budapest, 1968), p. 1549.
[18]F. H. Spedding and R. S. Bear, Phys. Rev. 39, 948 (1932); 42, 58 (1932); 44, 287 (1933); 46, 308 (1934).
[19]H. Lämmermann, Z. Phys. 150, 551 (1958); 160, 335 (1960); A. Friedrich, K. H. Hellwage, and H. Lämmermann, *ibid.* 159, 524 (1960).
[20]N. Rabbiner, Phys. Rev. 130, 502 (1963); J. Opt. Soc. Am. 57, 1376 (1967).
[21]L. F. Johnson, J. Appl. Phys. 34, 897 (1963).
[22]J. G. Gualtieri and T. R. AuCoin, J. Chem. Phys. 45, 4348 (1966); J. G. Gaultieri and G. P. de Lhery, *ibid.* 55, 1541 (1971).
[23]N. Karayianis and R. T. Farrar, J. Chem. Phys. 53, 3436 (1970).
[24]A. M. Morozov, D. E. Onopko, E. G. Reut, A. I. Ryskin, M. N. Tolstoy, and P. P. Feofilov, in Ref. 17, p. 1621.
[25]D. E. Wortman and D. Sanders, J. Chem. Phys. 53, 1247 (1970).
[26]G. R. Jones, J. Chem. Phys. 47, 4347 (1967).
[27]G. B. Finch and G. W. Clark, J. Chem. Phys. Solids 34, 922 (1973).
[28]G. E. Bleil and I. Broser, J. Phys. Chem. Solids 25, 11 (1964).
[29]M. J. Weber, Phys. Rev. B 4, 2932 (1971).
[30]R. K. Watts and H. J. Richter, Phys. Rev. B 6, 1584 (1972).
[31]J. P. van der Ziel, F. W. Ostermayer, and L. G. Van Uitert, Phys. Rev. B 2, 4432 (1970); J. P. van der Ziel, L. Kopf, and L. G. Van Uitert, *ibid.* 6, 615 (1972).
[32]N. Krasutsky and H. W. Moos, Phys. Rev. B 8, 1010 (1973).
[33]B. Blasse, Phillips Res. Rep. 24, 131 (1969).
[34]L. G. Van Uitert and L. F. Johnson, J. Chem. Phys. 44, 3514 (1966).
[35]T. Miyakawa and D. L. Dexter, Phys. Rev. B 1, 2961 (1970).
[36]R. Orbach, in *Optical Properties on Ions in Crystals*, edited by H. M. Crosswhite and H. W. Moos (Interscience, New York, 1967), p. 445; and presented at the NATO Institute on Optical Properties of Ions in Solids, Erice, Italy, 1974 (unpublished).
[37]F. A. Kroger, *Some Aspects of the Luminescence of Solids* (Elsevier, New York, 1948).
[38]Th. P. J. Botden, Phillips Res. Rep. 6, 425 (1951).
[39]G. K. Born, R. J. Grasser, and A. O. Scharmann, Phys. Status Solidi 28, 538 (1968); G. Born, A. Hofstaetter, A. Scharmann, and. G. Schawarz, J. Lumin. 1, 2 641 (1970).